Progress In Electromagnetics Research, Vol. 119, 265–277, 2011

DESIGN OF PLANAR ARRAYS COMPOSED BY AN ACTIVE DIPOLE ABOVE A GROUND PLANE WITH PARASITIC ELEMENTS

J. A. Rodríguez-González and F. Ares-Pena*

Dept. of Applied Physics, Univ. of Santiago de Compostela, 15782 Santiago de Compostela, Spain

Abstract—In this paper, several simple antenna designs based on the use of an active dipole placed above a ground plane with an array of parasitic dipoles are presented. The parasitic dipoles are used to modify the pattern of the active dipole yielding a pencil beam of moderate gain. The use of one active element provides a very simple feeding network that reduces the complexity of the antenna. The proposed technique optimizes the geometry and configuration of both active and parasitic elements. It is shown that the performance of the designed antennas is considerably better than that of a similar antenna without parasitic elements.

1. INTRODUCTION

Array antennas have been given increased attention for many radar and satellite applications due to their capabilities in controlling certain parameters of the pattern and their high efficiency [1, 2]. The main drawback of the arrays is the complexity and expensiveness of their feeding network. Recently, the use of parasitic arrays [3–11] illuminated by smaller active arrays has received some attention because they introduce degrees of freedom that allow patterns to be synthesized without modification of the active array feed. In [11], a technique for designing a planar array of parasitic dipoles that modify the pattern of a $\lambda/2$-dipole placed $\lambda/4$ over a ground plane was described. This method, that synthesizes a pencil beam pattern with good performance, uses the Particle Swarm Optimization (PSO) [12–20] tool of method of moments program FEKO [21] to optimize the

Received 11 July 2011, Accepted 28 July 2011, Scheduled 4 August 2011

* Corresponding author: Francisco Jose Ares-Pena (francisco.ares@usc.es).

length of each parasitic dipole and the distance between the planar array and the ground planes as well as the interspacing of the parasitic elements. In this model, the antenna works as a set of scattering elements in a mutual coupling environment localized in a plane. Each element, in the presence of others, acquires a phased-up trans-scattering capability. In a further work, this design was validated by means of a prototype, where experimental results showed a good agreement with the expected ones [22].

In this work, an innovative design based on the method described in [11] is presented. The antenna is composed of an active dipole placed above a double sided Printed Circuit Board (PCB), where the lower side acts as a ground plane and the above side contains the parasitic elements that allows to reconfigure the power pattern of the active dipole. The coupling between the active dipole and the parasitic array, as well as the coupling between the parasitic elements, increases the effective antenna surface. We will show that the antenna has a performance substantially better than the obtained without parasitic elements. An additional design that uses two layers of parasitic dipoles is also presented: in this case, the design above described is used as a feeder of an additional array of parasitic dipoles.

2. THE METHOD

The antenna system is composed by two parts: i) a double sided PCB with two copper layers laminated onto a dielectric substrate: the lower side acts as a ground plane and the above side contains a planar array of parasitic dipoles of lengths $l_{i,j}$ and separated Δx_i along the X-axis, and Δy_j along the Y-axis; ii) one $\lambda/2$ active dipole placed above the PCB at a distance Δz (see Fig. 1).

The proposed method is based on the optimization of the array geometry in order to obtain a high directivity pattern. This optimization is performed by means of the PSO tool of program FEKO that takes into account the mutual coupling between all the parasitic and active elements as well as the presence of the dielectric substrate.

A uniformly spaced planar array of parasitic dipoles of length $\lambda/2$ is considered as a starting point in the optimization process. In this procedure, the length of each parasitic dipole $l_{i,j}$, the distance between the active dipole and the planar array (Δz), and the interspacing in the Y-axis direction (Δy_j) of the parasitic array (see Fig. 1) are modified. As in [11], the interspacing in the X-axis (Δx_i) is fixed to 0.55λ for all elements (we found than the optimal value calculated by PSO was always the smallest as possible) and we consider quadrantal symmetry for the parasitic array what reduces the number of unknowns.

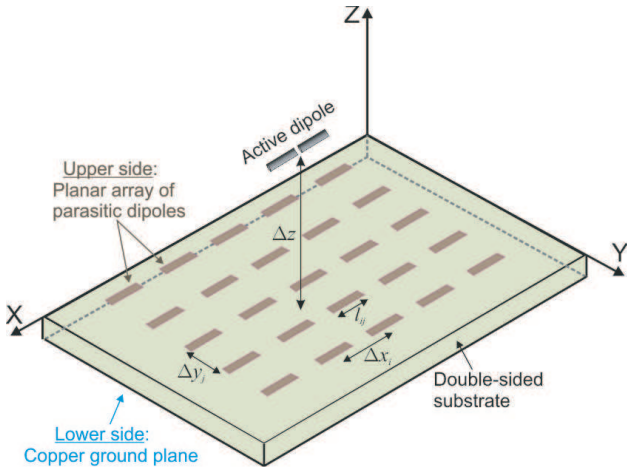

Figure 1. Geometry of the antenna composed by an active dipole in front of a double-sided substrate: the upper side contains a planar array of parasitic dipoles and the lower one is a conductor that acts as a ground plane.

The variables above mentioned were optimized by means of PSO to minimize a cost function consisting of a term to increase directivity in the broadside ($\theta = 0°$, $\phi = 0°$):

$$C = 1/directivity \tag{1}$$

After the optimization process, the obtained antenna geometry is simulated by evaluating the induced currents in each parasitic element: those dipoles resulting with very low induced currents are removed from the array after checking that their elimination does not reduced the antenna performance. This array thinning allows the simplification of the antenna geometry.

By combining the above antenna with the described in [11], we proposed a new design in which an additional array of parasitic dipoles is placed above the antenna system of Fig. 1. The optimization process is similar to above, but it is necessary to take into account the additional unknowns of the second parasitic array. This design will significantly improve the antenna performance, as the Section 3.3 reports.

3. DESIGN EXAMPLES

3.1. Active Dipole above a Planar Array of Parasitic Dipoles with Uniform Interelement Spacing

The antenna of the first design is composed by a $\lambda/2$ active dipole above a planar array of 48 parasitic dipoles. In the simulation, the substrate of the double sided PCB is DICLAD 880 ($\varepsilon_r = 2.17$, $\tan\delta = 0.0009$) of thickness 0.05 inches. In this example, we will also consider uniform spacing in the Y-axis direction for all the parasitic elements, so the unknowns for the optimization process are: the dipole lengths (l_{ij}), the interelement spacing in the Y-axis direction (Δy), and the distance between the active dipole and the planar array (Δz). After the PSO-based optimization process, the array geometry shown in Fig. 2 is obtained. The total size of the planar array is $4.60\lambda \times 3.67\lambda$, with $\Delta y = 0.41\lambda$ and it is located at $\Delta z = 1.22\lambda$ below the active dipole. The radiation pattern obtained (see Fig. 2), has a directivity of 17.36 dBi and a side lobe level, SLL, of -9.63 dB. An analysis of the induced currents in each parasitic element reveals that, in this design, there are no weakly excited elements to be removed in a further array thinning without affecting to the antenna performance.

An analysis of the bandwidth with FEKO [21] reveals a value of 2.54% for the 3 dBi absolute gain bandwidth (Fig. 3). The absolute gain of this figure has been calculated considering that the feeding dipole is matched to the generator at the central frequency. Calculation

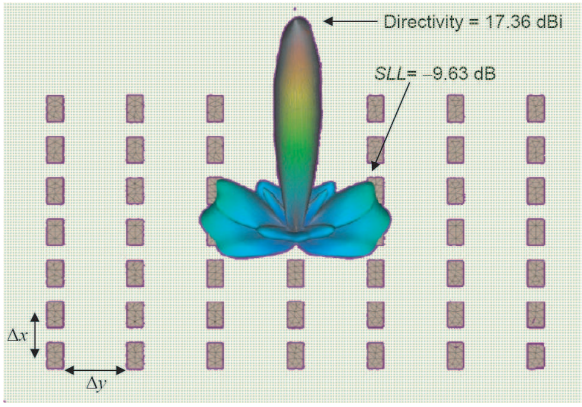

Figure 2. Geometry and power pattern radiated by the antenna composed of a $\lambda/2$ active dipole placed above a planar array of 48 parasitic elements with uniform interelement spacing in the Y-axis ($\Delta y = \text{cte}$).

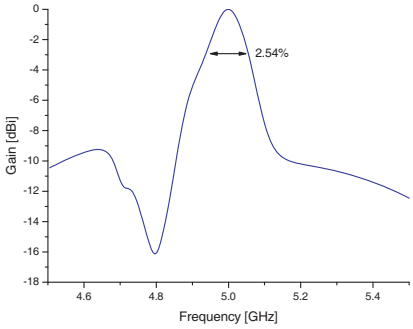

Figure 3. Antenna gain versus frequency for the antenna of Fig. 2.

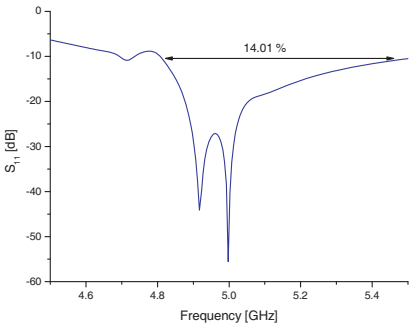

Figure 4. Magnitude of the input reflection coefficient versus frequency for the antenna of Fig. 2.

of the input reflection coefficient S_{11}, revealed a bandwidth of 14.01% at -10 dB (Fig. 4).

3.2. Active Dipole above a Planar Array of Parasitic Dipoles with Non Uniform Interelement Spacing in the Y-axis Direction

It is possible to improve the antenna performance of the previous design by introducing additional degrees of freedom in the antenna geometry during the optimization process. In this case, we will consider a non-uniform interelement spacing in the Y-axis direction of the parasitic array (Δy_{i}). With this consideration and using the same design parameters as above, the array geometry shown in Fig. 5 is obtained after the PSO optimization. The total size of the planar array is $5.06\lambda \times 3.76\lambda$, with $\Delta y_1 = 0.45\lambda$, $\Delta y_2 = 0.33\lambda$ y $\Delta y_3 = 0.58\lambda$, and it is located at $\Delta z = 1.23\lambda$ below the active dipole. These values have been calculated during the optimization process without imposing any kind of restriction to the antenna geometry. The radiation pattern obtained (see Fig. 5), has a directivity of 18.33 dBi and a side lobe level, SLL, of -10.92 dB. Comparing these results with those of the previous design (see Table 1), we have obtained an improvement of 1 dBi and 1.3 dB in the directivity and the side lobe level, respectively.

In this case, the bandwidth analysis reveals a value of 1.94% for the 3 dBi absolute gain bandwidth (Fig. 6). Calculation of the input reflection coefficient S_{11}, revealed a bandwidth of 15.8% at -10 dB (Fig. 7). Comparing these results with the results of the previous design (see Table 1), we show that this new design show a slightly less bandwidth in terms of gain but a better one in terms of S_{11}.

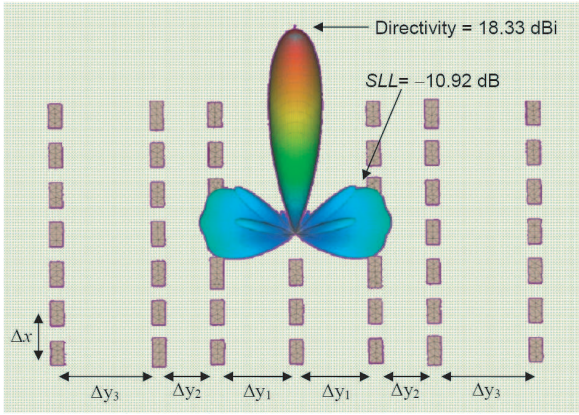

Figure 5. Geometry and power pattern radiated by the antenna composed of a $\lambda/2$ active dipole placed above a planar array of 48 parasitic elements with a non-uniform interelement spacing in the Y-axis.

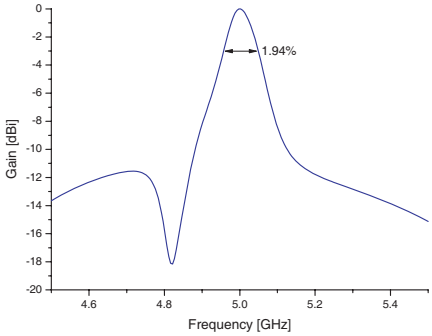

Figure 6. Antenna gain versus frequency for the antenna of Fig. 5.

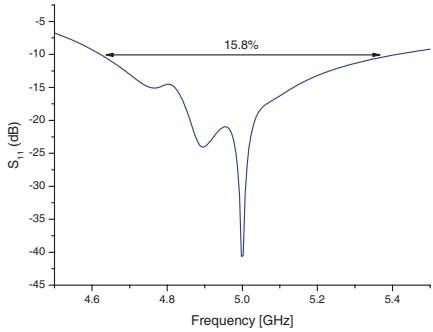

Figure 7. Magnitude of the input reflection coefficient versus frequency for the antenna of Fig. 5.

After the optimization process, a simulation is done for analyzing the induced currents in each parasitic element. In this particular example, 15 parasitic elements have practically null currents, so these elements are removed. A further simulation of the resulting antenna with this reduced geometry shows that the performance of the initial antenna is almost unaffected by this thinning. The final geometry of the parasitic array is shown in Fig. 8. Note that the active dipole is close to the front of some of the elements removed in the array

thinning: due to the location of these elements, their field pattern would be blocked by the feeder reducing the antenna directivity. The PSO optimization calculates the appropriate geometry of these dipoles in order to minimize their field and thus minimize the blocking effects.

Starting with the antenna geometry obtained in the previous example, a study modifying the height of the active dipole above the parasitic array Δz, is shown in Fig. 9. Although the maximum value corresponds to a distance of $\Delta z = 1.23\lambda$ obtained in the previous design, it is possible to reduce the antenna height to 0.6λ at the expense of reducing the antenna gain to 13.4 dBi. This adds flexibility to our design and can be interesting in order to increase the antenna compactness.

In order to study the influence of the parasitic array in antenna performance, a $\lambda/2$-dipole located at a distance of $\lambda/4$ above a ground plane was simulated with FEKO. In this case the directivity of the power pattern is 7.51 dBi, so the parasitic array used in the proposed method achieves an improvement of 10.82 dBi in terms of directivity. In the simulation, we found that considering a ground plane of dimensions greater than $1\lambda \times 1\lambda$ does not improve the performance of the pattern radiated by the dipole. The conclusion to be drawn is that the couplings between the parasitic array dipoles increase the effective antenna size and thus the pattern directivity. This design can be considered as a good performance feeder of a more complex antenna, as we will show in the following example.

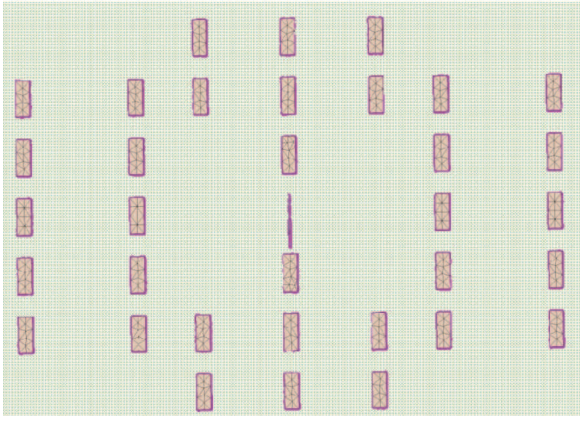

Figure 8. Final geometry of the antenna of Fig. 3 after removing 15 weakly excited elements.

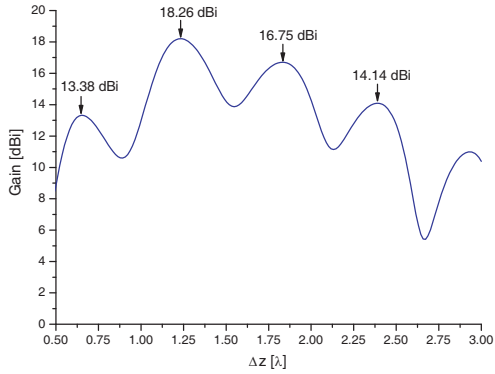

Figure 9. Antenna gain versus the distance between the active dipole and the planar array Δz.

3.3. Active Dipole between two Parasitic Arrays with Uniform Interelement Spacing

In the last example, we combine the design obtained in the previous section with the design described in [11]. In this new design, an additional layer of 49 parasitic dipoles is placed above the antenna shown in Fig. 1 in order to reconfigure the radiation pattern and increase the directivity. As in the previous case, we consider a double sided PCB of DICLAD 880 in the antenna bottom, whereas in the top a substrate of FR4 ($\varepsilon_{\mathrm{r}} = 4.6$, $\tan\delta = 0.014$) of thickness 0.06 inches is considered in order to guarantee an acceptable stiffness of the additional array. The optimization process is similar to above, but it is necessary to take into account the additional unknowns of the second parasitic array: the length of these parasitic elements l'_{ij}, their $\Delta y'$ spacing and the distance $\Delta z'$ between the two parasitic arrays. As in the previous sections, the interelement spacings in the X-axis have been fixed to the value $\Delta x = \Delta x' = 0.55\lambda$. On the other hand, the interelement spacings in the Y-axis direction are uniform in both arrays, although they are calculated during the PSO optimization. The antenna geometry is shown in Fig. 10.

After the PSO-based optimization process, the antenna geometry shown in Fig. 11 is obtained. The planar array on the bottom has a total size of $4.14\lambda \times 3.80\lambda$, with $\Delta y = 0.69\lambda$ and it is located at $\Delta z = 0.76\lambda$ below the active dipole, where the planar array on the top has a total size of $5.86\lambda \times 3.64\lambda$, with $\Delta y' = 0.94\lambda$ and is separated 1.23λ of the first array ($\Delta z'$). The radiation pattern obtained (see Fig. 11), has a directivity of 24.21 dBi and a side lobe level, *SLL*, of

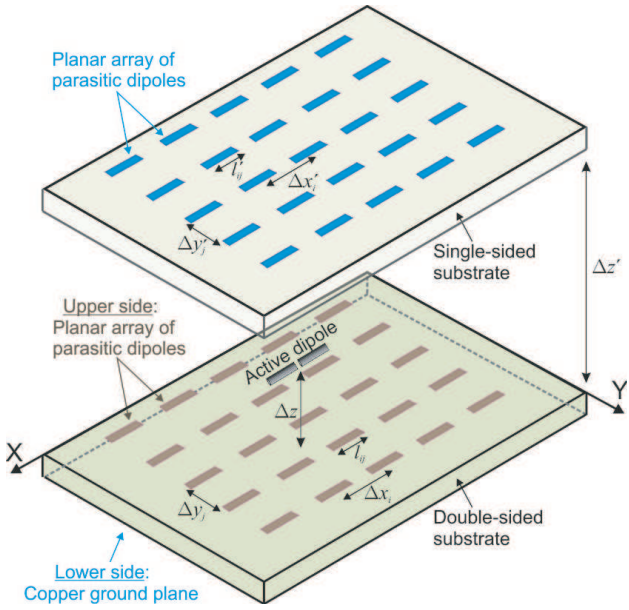

Figure 10. Geometry of the antenna composed by an active dipole between two arrays of parasitic dipoles.

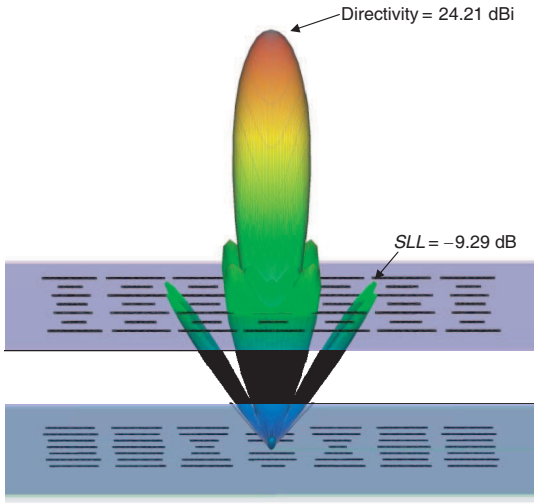

Figure 11. Geometry and power pattern radiated by the antenna composed of a $\lambda/2$ active dipole placed between two arrays of parasitic dipoles.

Table 1. Summary of the geometry and performance parameters of the antennas designed in Section 3. Results of a $\lambda/2$-dipole $\lambda/4$ above a ground plane are included for comparison.

	Array Size	Height to the feeder (Δz) [λ]	Direct. [dBi]	SLL [dB]	Bandwidth	
					3 dB-Gain	10 dB-S_{11}
$\lambda/2$-dipole above a planar array of parasitic dipoles with uniform interlement spacing (Fig. 2)	$4.60\lambda \times 3.67\lambda$	1.22	17.36	-9.63	2.54%	14.01%
$\lambda/2$-dipole above a planar array of parasitic dipoles with non uniform interlement spacing (Fig. 5)	$5.06\lambda \times 3.76\lambda$	1.23	18.33	-10.92	1.94%	15.80%
$\lambda/2$-dipole between two parasitic arrays (Fig. 11)	$4.14\lambda \times 3.80\lambda$ $5.86\lambda \times 3.64\lambda$	0.76 ($\Delta z' = 1.23\lambda$)	24.21	-9.29	3.26%	29.15%
$\lambda/2$-dipole above a ground plane	-	0.25	7.51	-	23.3%	11.2%

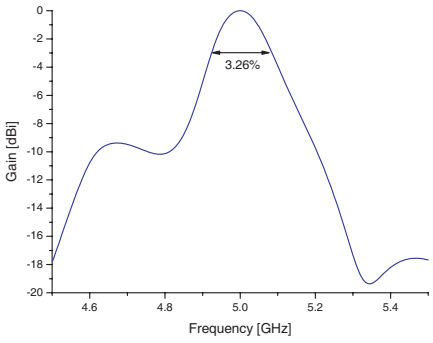

Figure 12. Antenna gain versus frequency for the antenna of Fig. 11.

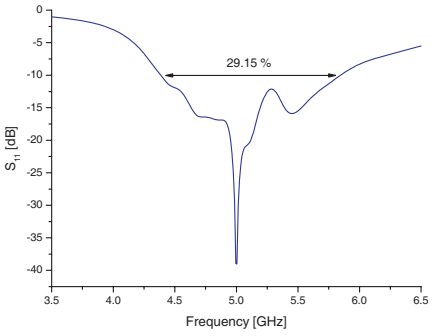

Figure 13. Magnitude of the input reflection coefficient versus frequency for the antenna of Fig. 11.

−9.29 dB. Comparing these results with those of the previous section (see Table 1), we have found that the use of the additional layer increased the directivity in 6.8 dBi.

An analysis of the bandwidth reveals a value of 3.26% for the 3 dBi absolute gain bandwidth (Fig. 12). Calculation of the input reflection coefficient S_{11}, revealed a bandwidth of 29.15% at −10 dB (Fig. 13). All of these values are substantially better than the obtained in the previous designs (see Table 1).

4. CONCLUSIONS

Several simple antenna designs based on the use of an active dipole placed above a ground plane with an array of parasitic dipoles have been presented. The presence of the parasitic dipoles increases the effective antenna size and allows a significant improvement over the directivity of an isolated dipole in front of a ground plane. The use of only one active element provides a very simple feeding network that reduces the complexity of the antenna. We have found that by using this configuration to feed an additional layer of parasitic dipoles, it is possible to increase substantially the antenna performance. Although the presence of two layers of parasitic arrays increases the antenna complexity, it could be necessary and justifiable in applications requiring a higher directivity and/or bandwidth.

ACKNOWLEDGMENT

This work has been supported by the Spanish Ministry of Education and Science under Project TEC2008-04485 and by the Xunta de Galicia under Project 09TIC006206PR.

REFERENCES

1. Mailloux, R. J., *Phased Array Antenna Handbook*, 2nd edition, Artech House, Inc., 2005.
2. Hansen, R. C., *Phased Array Antennas,* John Wiley & Sons, Inc., 1998.
3. Yuan, H.-W., S.-X. Gong, P.-F. Zhang, and X. Wang, "Wide scanning phased array antenna using printed dipole antennas with parasitic element," *Progress In Electromagnetics Research Letters*, Vol. 2, 198–193, 2008.

4. Ares-Pena, F. J., G. Franceschetti, and J. A. Rodriguez, "A simple alternative for beam reconfiguration of array antennas," *Progress In Electromagnetics Research*, Vol. 88, 227–240, 2008.
5. Álvarez-Folgueiras, M., J. A. Rodríguez González, and F. Ares-Pena, "Low-sidelobe patterns from small, low-loss uniformly fed linear arrays illuminating parasitic dipoles," *IEEE Trans. Antennas Propagat.*, Vol. 57, No. 5, 1583–1585, 2009.
6. Chen, X., G. Fu, S. X. Gong, J. Chen, and X. Lu, "A novel microstrip array antenna with coplanar parasitic elements for UHF RFID reader," *Journal of Electromagnetic Waves and Applications,* Vol. 23, Nos. 17–18, 2491–2502, 2009.
7. Kamarudin, M. R. B. and P. S. Hall, "Switched beam antenna array with parasitic elements," *Progress In Electromagnetics Research B*, Vol. 13, 187–201, 2009.
8. Zhang, M., Y.-Z. Yin, J. Ma, Y. Wang, W.-C. Xiao, and X.-J. Liu, "A racket-shaped slot UWB antenna coupled with parasitic strips for band-notched application," *Progress In Electromagnetics Research Letters*, Vol. 16, 35–44, 2010.
9. Tu, Z.-H., Q.-X. Chu, and Q.-Y. Zhang, "High-gain slot antenna with parasitic patch and windowed metallic superstrate," *Progress In Electromagnetics Research Letters*, Vol. 15, 27–36, 2010.
10. Zhao, K., S. Zhang, and S. He, "Enhance the bandwidth of a rotated rhombus slot antenna with muliple parasitic elements," *Journal of Electromagnetic Waves and Applications,* Vol. 24, Nos. 14–15, 2087–2094, 2010.
11. Álvarez-Folgueiras, M., J. A. Rodríguez-González, and F. Ares-Pena, "Pencil beam patterns obtained by planar arrays of parasitic dipoles fed by only one active element," *Progress In Electromagnetics Research*, Vol. 103, 419–431, 2010.
12. Pathak, N. N., G. K. Mahanti, S. K. Singh, J. K. Mishra, and A. Chakraborty, "Synthesis of thinned planar circular array antennas using modified particle swarm optimization," *Progress In Electromagnetics Research Letters*, Vol. 12, 87–97, 2009.
13. Mangoud, M. A.-A. and H. M. Elragal, "Antenna array pattern synthesis and wide null control using enhanced particle swarm optimization," *Progress In Electromagnetics Research B*, Vol. 17, 1–14, 2009.
14. Khodier, M. M. and M. Al-Aqeel, "Linear and circular array optimization: A study using particle swarm intelligence," *Progress In Electromagnetics Research B*, Vol. 15, 347–373, 2009.

15. Benedetti, M., G. Oliveri, P. Rocca, and A. Massa, "A fully-adaptive smart antenna prototype: Ideal model and experimental validation in complex interference scenarios," *Progress In Electromagnetic Research*, Vol. 96, 173–191, 2009.
16. Zhang, S., S.-X, Gong, and P.-F. Zhang, "A modified PSO for low sidelobe concentric ring arrays synthesis with multiple constraints," *Journal of Electromagnetic Waves and Applications*, Vol. 23, Nos. 11–12, 1535–1544, 2009.
17. Zhang, L., F. Yang, and A. Z. Elsherbeni, "On the use of random variables in particle swarm optimizations: A comparative study of Gaussian and uniform distributions," *Journal of Electromagnetic Waves and Applications*, Vol. 23, Nos. 5–6, 771–721, 2010.
18. Rocca, P., L. Poli, G. Oliveri, and A. Massa, "Synthesis of time-modulated planar arrays with controlled harmonic radiations," *Journal of Electromagnetic Waves and Applications*, Vol. 24, Nos. 5–6, 827–838, 2010.
19. Carro Ceballos, P. L., J. De Mingo Sanz, and P. G. Dúcar, "Radiation pattern synthesis for maximum mean effective gain with spherical wave expansions and particle swarm techniques," *Progress In Electromagnetics Research*, Vol. 103, 355–370, 2010.
20. Barkat, O. and A. Benghalia, "Synthesis of superconducting circular antennas placed on circular array using a particle swarm optimisation and the full-wave method," *Progress In Electromagnetics Research B*, Vol. 22, 103–119, 2010.
21. EM Software and Systems, FEKO Suite 5.4, 2008, www.feko.info.
22. Álvarez-Folgueiras, M., J. A. Rodríguez-González, and F. Ares-Pena, "Experimental results on a planar array of parasitic dipoles fed by one active element," *Progress In Electromagnetics Research*, Vol. 113, 369–377, 2011.